https://doi.org/10.37434/tpwj2021.06.01

MODELING OF STRESS-STRAIN STATES OF AMg6 ALLOY DUE TO IMPACT ACTION OF ELECTRODE-INDENTER IN ELECTRODYNAMIC TREATMENT

L.M. Lobanov[1], **M.O. Pashchyn**[1], **O.L. Mikhodui**[1], **P.V. Goncharov**[1], **Yu.M. Sydorenko**[2] and **P.R. Ustymenko**[2]

[1]E.O. Paton Electric Welding Institute of the NAS of Ukraine
11 Kazymyr Malevych Str., 03150, Kyiv, Ukraine. E-mail: office@paton.kiev.ua
[2]National Technical University of Ukraine «Igor Sikorsky Kyiv Polytechnic Institute»
37 Peremohy Prosp., 03056, Kyiv, Ukraine

The calculated model of the process of impact interaction of the electrode-indenter with the plate of aluminium AMg6 alloy during electrodynamic treatment is presented. The solution of the problem is carried out on the basis of the Prantle–Reiss relations for the movement of an elastic-plastic medium in a plane two-dimensional Lagrangian formulation using the software «ANSYS/LS-DYNA». The results of calculating the process of forming areas of residual stresses and plastic deformations under the impact action of the indenter are presented. It was found that under the impact action of the indenter at a speed of 10 m/s on the reverse surface of the plate of AMg6 alloy, the values of plastic deformations are higher than on the contact one. This is explained by the effect of reflection of a plastically deformed layer of metal from the back side of the plate, which stays in the conditions of resting on a rigid support. An experimental verification of the model adequacy during evaluation of the distribution of plastic deformations after electrodynamic treatment of a welded plate of AMg6 alloy was performed. 16 Ref., 2 Tables, 9 Figures.

Keywords: electrodynamic treatment, aluminium alloy, impact interaction, mathematical modeling, residual stresses, plastic deformations, electrode-indenter, movement, elastic-plastic medium

Welding, which is one of the main technological processes in mechanical engineering, shipbuilding and construction, causes residual tensile stresses in structures, the peak values of which are close to the yield strength of metal. Residual stresses have a negative effect on the accuracy of welded parts, causing residual deformations of bending, twisting and longitudinal reduction in area in the latter. These stresses also have a negative effect on the fatigue strength and corrosion resistance of both welded joints and a structure as a whole [1]. To eliminate residual welding stresses and deformations, appropriate designing and technological measures are used, for example, different methods of postweld treatment of metal structures [2].

One of the promising technological methods of stress-strain state control is electrodynamic treatment (EDT) of welded aircraft and shipbuilding structures of light alloys [3, 4]. The principle of EDT effect is based on the joint action of two factors on a welded joint — pulsed electric current and dynamic pressure. In [5], the results of experimental studies of EDT effect on the stress-strain state of welded joints of aluminium AMg6 alloy are described. It is shown that EDT initiates plastic tensile deformations in metal. The result of their interaction with residual (plastic) welding compression deformations is a reduction of residual stresses in a welded joint.

At the same time, the experimental method of evaluating the efficiency of EDT, which is described in [6], is quite difficult to use for finding the optimal modes of treatment of a wide range of metals, alloys and welded joints. This is associated with the consideration and evaluation of a large number of technological variants of EDT for compliance with the established optimization criterion — reduction of residual welding stresses to a set level.

In addition, to determine the direction of EDT improvement, it is necessary to have information about parameters of the stress-strain state over the thickness of structural elements to be welded. It is quite difficult to obtain such information experimentally using existing procedures, because usually the zones of stress registration are located on the outer surfaces of welded structures [7]. Therefore, the most appropriate way to solve this problem is to use the methods of mathematical modeling.

The aim of the work is to develop a method and an appropriate mathematical model for evaluation of

L.M. Lobanov — https://orcid.org/0000-0001-9296-2335, M.O. Pashchyn — https://orcid.org/0000-0002-2201-5137,
O.L. Mikhodui — https://orcid.org/0000-0001-6660-7540

stress-strain state of plates of aluminium AMg6 alloy from the influence of the EDT component — impact action of the electrode-indenter.

Investigation procedure. Creation of dynamic pressure on surfaces of the plates treated by EDT, is carried out according to the scheme presented in Figure 1. The specimens *4* treated by EDT, in the form of plates are located on the table *5*. Using an electrical circuit of the installation containing the capacitor C and the inductor *1*, a magnetic field of appropriate power is generated. Under the action of this field, the disc *2* together with the electrode-indenter *3* receive different values of the initial speed of movement (V_0) in the direction of the table *5*. The values of V_0 were chosen on the basis of previous studies, the results of which established a correlation between the growth rate of the pulse current values in EDT and V_0. The impact interaction of the EDT electrode-indenter with the surface of the plates leads to the formation of a wide range of stress-strain states depending on the value of V_0. It should be noted that in this work the impact interaction of the EDT electrode-electrode with the plate is considered, which stays in the unstressed state, i.e. residual stresses are absent in it.

The creation of a mathematical model of the process described above should be carried out using a simplified two-dimensional (2D) flat formulation. The calculated scheme of the problem concerning the process of impact interaction of the electrode-indenter with the plates is presented in Figure 2.

The solution of the problem was performed using the software ANSYS/LS-DYNA [8, 9]. To plot a finite element grid (FEG) of the problem, a flat two-dimensional finite element in the form of a rectangle SOLID 162 was used.

Given that this problem considers the stress-strain state of solids, then computer modelling should be performed using the Lagrangian approach [10–12]. As is known, the Lagrangian approach uses a movable finite-element grid, which is rigidly connected to the medium and deformed together with it.

The presence of the geometric symmetry of the impact-interacting bodies described above allows considering only half of their cross-section with a simultaneous imposition of the corresponding boundary conditions on it. These conditions include the imposition of a ban on the movement of nodes of FEG bodies on the axis of symmetry in the horizontal direction *X*. The presence of the plates of the working table *5* (Figure 1) in the scheme of electrodynamic treatment should be replaced by resting on an absolutely rigid base *3* (Figure 2), which in the mathematical formulation will be equivalent to the imposition of a ban on movement in the vertical direction of *Y* FEG nodes,

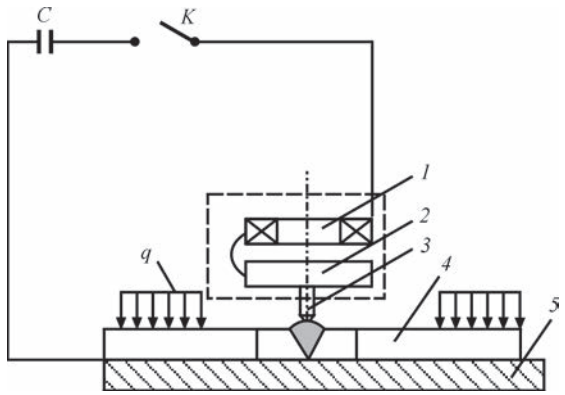

Figure 1. Scheme of electrodynamic treatment of plates: *1* — inductor; *2* — disc; *3* — movable electrode-indenter; *4* — treated specimen; *5* — working table; *q* — load that fixes the specimen

that belong to the lower surface of the plate contacting with the table.

The experience in solving problems of such a class shows that a number of rows (layers) of finite elements per a unit of thickness of a metal plate should be at least ten [13]. Therefore, to construct a finite-element model of the plate and the electrode-indenter, a finite element with a maximum characteristic size of 0.1 mm was chosen. The plotted FEG of the problem with a finite element of such a characteristic size had the following characteristics: number (pcs) of finite elements — 128203; nodes — 131042.

For numerical modeling of high-speed impact processes in most practical problems, continuum models (macromodels) of the studied medium are used [11]. The basis of macromodels is the hypothesis about continuity of changes in the characteristics of the medium in space (coordinate, time), which allows writing the laws of conservation of mass, amount of movement and energy in the form of differential equations in partial derivatives.

If we choose a Cartesian (rectangular) coordinate system to describe the adiabatic movement of an elastic-plastic medium with a density ρ (kg/m^3), then the

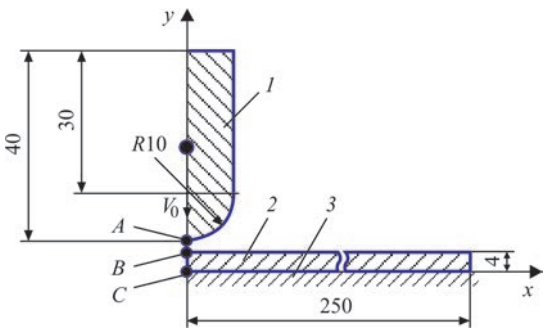

Figure 2. Calculated scheme of the process of dynamic load of plates, which are treated by EDT: *1* — electrode-indenter; *2* — treated specimen; *3* — absolutely rigid base; *A* — point on the outer surface of the electrode-indenter; *B* — plates; *C* — on the reverse surface of the plate

system of corresponding equations in the two-dimensional formulation will have the following form [14]:

• the continuity equation:

$$\frac{d\rho}{dt}+\rho\left(\frac{\partial u}{\partial x}+\frac{\partial v}{\partial y}\right)=0,$$

where u, v are the components of the velocity vector of the medium movement, m/s;

• equation of medium movement:

$$\rho\frac{du}{dt}=\frac{\partial\sigma_{xx}}{\partial x}+\frac{\partial\sigma_{xy}}{\partial y},\quad \frac{dv}{dt}=\frac{\partial\sigma_{yx}}{\partial x}+\frac{\partial\sigma_{yy}}{\partial y},$$

where σ_{ij} are the components of the stress tensor, PA;

• energy equation for a unit of mass:

$$\rho\frac{dE^*}{dt}=\sigma_{xx}\dot{\varepsilon}_{xx}+\sigma_{yy}\dot{\varepsilon}_{yy}+2\sigma_{xy}\dot{\varepsilon}_{xy},$$

$$\dot{\varepsilon}_{xx}=\frac{\partial u}{\partial x},\quad \dot{\varepsilon}_{yy}=\frac{\partial v}{\partial y},\quad \dot{\varepsilon}_{xy}=\frac{1}{2}\left(\frac{\partial u}{\partial y}+\frac{\partial v}{\partial x}\right),$$

where $\dot{\varepsilon}_{ij}=\frac{d\varepsilon_{ij}}{dt}$ are the components of the strain rate tensor, s^{-1}.

To study the processes, associated with large plastic deformations of medium, finite deformations and the theory of plastic flow are used. This theory considers the plastic deformation of a solid as a state of movement. The corresponding Prandtl–Reiss ratios can be written as follows:

$$\frac{dD_{\sigma_{xx}}}{dt}+2G\dot{\lambda}D_{\sigma_{xx}}=2G\left(\dot{\varepsilon}_{xx}+\frac{1}{3\rho}\frac{d\rho}{dt}\right),$$

$$\frac{dD_{\sigma_{yy}}}{dt}+2G\dot{\lambda}D_{\sigma_{yy}}=2G\left(\dot{\varepsilon}_{yy}+\frac{1}{3\rho}\frac{d\rho}{dt}\right),$$

$$\frac{dD_{\sigma_{xy}}}{dt}+2G\dot{\lambda}D_{\sigma_{xy}}=2G\dot{\varepsilon}_{xy},$$

where G is the shear modulus, Pa; $D_{\sigma_{ij}}$ are the components of stress deviator, then

$$D_{\sigma_{ij}}=\sigma_{ij}+p\delta_{ij},\delta_{ij}=1(i=j),\delta_{ij}=0(i\neq j),$$

where p, the average normal stress (Pa), has the following form:

Table 1. Calculated time of interaction of the electrode-indenter with the plate

Speed of movement of the electrode-indenter V_0, m/s	Contact time, μs		
	Start	Finish	Duration
1	96	172	76
5	20	106	86
10	10	112	102

$$p=-\frac{\sigma_x+\sigma_y+\sigma_z}{3}.$$

The value of the specific power of plastic deformation is determined as:

$$\dot{\lambda}=\frac{3}{2Y^2}\sigma_{ij}\dot{\varepsilon}^p_{ij},\left(\frac{1}{\text{Pa}\cdot\text{s}}\right),$$

where Y is the dynamic yield strength of the material being studied.

The system of equations is closed by the equation of medium condition in the form:

$$p=p(\rho,E).$$

In the mathematical formulation, the behavior of materials of the plate (aluminium AMg6 alloy) and the electrode-indenter (copper M1) under the action of external pulse load was described using an ideal elastic-plastic rheological model of the material, which in the material library of the ANSYS/LS-DYNA software is called PLASTIC-KINEMATIC. For this model, the value of the dynamic yield strength of the material (Y) was taken equal to the value of the yield strength (σ_y). The corresponding values of the parameters of this model in the work were taken as follows:

• plate with the sizes of 500×500×4 mm of aluminium AMg6 alloy:
density (ρ), kg/m³ 2640
modulus of elasticity (E), GPa 71
Poisson's ratio (μ) 0.34
yield strength (σ_y), MPa 150

• electrode indenter of copper M1 alloy of 102.5 g receives three values of V_0, namely, 1, 5 and 10 m/s:
density (ρ), kg/m³ 8940
modulus of elasticity (E), GPa 128
Poisson's ratio (μ) 0.35
yield strength (σ_y) MPa 300

Over the whole area of the movement of ideally-plastic medium, the relation has to be carried out, which represents a condition of von Mises yield:

$$D^2_{\sigma_1}+D^2_{\sigma_2}+D^2_{\sigma_3}\leq\frac{2}{3}Y^2,$$

where D_{σ_1}, D_{σ_2}, D_{σ_3} are the main components of the stress deviator, Pa.

Results of mathematical modeling and their discussion. The performed numerical analysis showed differences in the process of interaction of the plate *2* and the electrode-indenter *1* (Figure 2) at different values of its initial movement speed (Table 1).

From Table 1 it is seen, that an increase in V_0 from 1 to 10 m/s increases the time of contact interaction of bodies by 35 %. As a result, a different indenta-

tion depth of the electrode-indenter in the plate was formed.

The indentation depth was calculated as a value of vertical movement along the impact line of the point *B*, which is located on the outer surface of the plate on the axis of symmetry *y* (Figure 2):

$$y = y_0 - y_c,$$

where y_0 is the initial coordinate of the point *B* till the moment of interaction of bodies, mm; y_c is the value of the coordinate of the point *B* after the interaction of bodies, mm.

The calculated values of the indentation depth of the indenter in the plate are presented in Table 2.

From Table 2 it is seen, that a different value of the depth Δy resulted in the formation of different sizes of the zone of effective plastic deformation $\varepsilon^p_{\text{eff}}$, which was determined by the formula:

$$\varepsilon^p_{\text{eff}} = \frac{\sqrt{2}}{3}\sqrt{(\varepsilon_1 - \varepsilon_2)^2 + (\varepsilon_2 - \varepsilon_3)^2 + (\varepsilon_3 - \varepsilon_1)^2},$$

where ε_1, ε_2, ε_3 are the main deformations.

It should be noted here that the depth of the zone of plastic deformations (*y*) is measured from the contact surface of the plate along the impact line. The value of the width of the zone (*x*) (Table 2) is calculated from the axis of symmetry of the problem in the horizontal direction *x* (Figure 2) and is indicated without taking into account the symmetry of the problem.

Table 2. Calculated parameters of the zone of effective plastic deformation

Speed of movement of the electrode-indenter (V_0), m/s	Indentation depth (Δy), mm	Depth of zone (y), mm	Width of zone (x), mm	Maximum value $\varepsilon^p_{\text{eff}}$
1	0.02	0.46	0.68	0.076
5	0.17	1.95	1.96	0.174
10	0.46	4.00	2.97	0.238

Time stages (kinetics) of formation of the zone of effective plastic deformations ($\varepsilon^p_{\text{eff}}$, *c*) of the plate over its entire thickness at the moment of contact with the electrode-indenter, moving at a speed V_0 = 10 m/s, is shown in Figure 3. From the Figure it is seen that at 20 μs of the process of interaction of the indenter with the plate, the shape of the profile of the zone of effective plastic deformations resembles the shape of a circular segment (Figure 3, *a*). The value $\varepsilon^p_{\text{eff}}$ currently reaches a value of 0.15. At 40 μs of the process

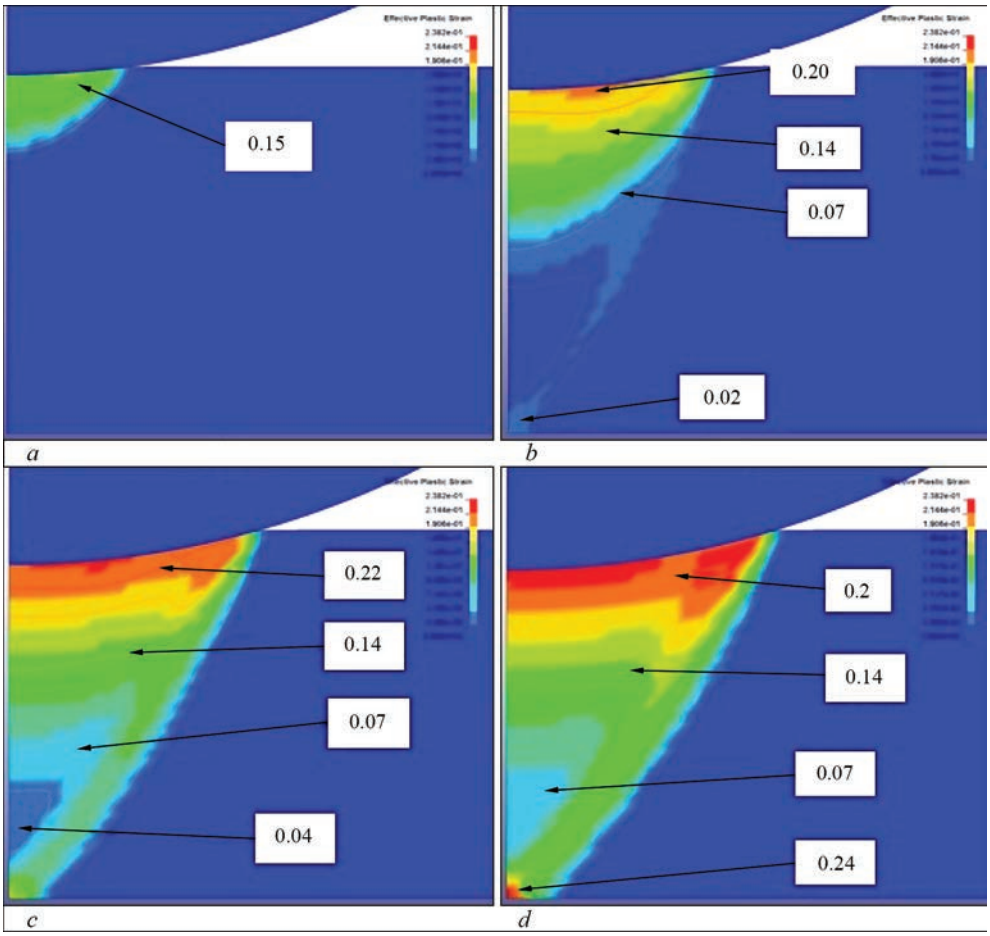

Figure 3. Process of forming a zone of effective plastic deformations $\varepsilon^p_{\text{eff}}$ in the plate (indenter speed is 10 m/s) in the period of time, μs: *a* — 20; *b* — 40; *c* — 60; *d* — 80

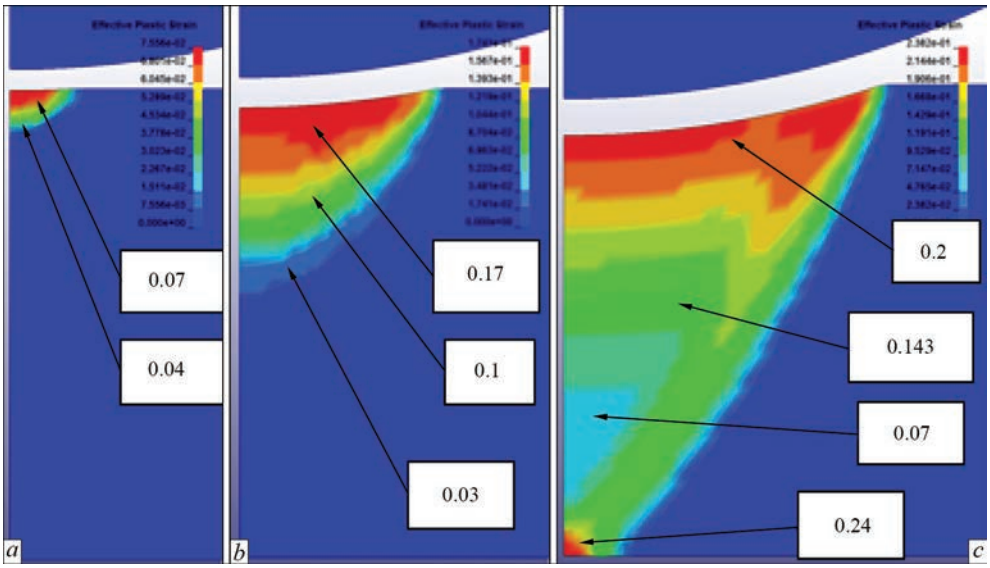

Figure 4. Residual calculated distribution of effective plastic deformations in the middle of the plate at different values of collision rate with the electrode-indenter, m/s: *a* — 1; *b* — 5; *c* — 10

(Figure 3, *b*), the boundaries of this zone go to the reverse surface of the plate. It means, that the electrode-indenter needed 30 μs to form a zone of plastic deformations over the entire thickness of the plate (period from 10 μs (Table 1) to 40 μs (Figure 3, *b*)). At this moment, the value $\varepsilon^p_{\text{eff}}$ grows by 25 % to $\varepsilon^p_{\text{eff}}$ = = 0.20. Further (60, 80 μs) the shape of the profile of the zone is transformed from a triangular (Figure 3, *b*) to a trapezoidal shape with an increase of $\varepsilon^p_{\text{eff}}$ to 0.22 and 24, respectively (Figure 3, *c*, *d*).

At the same time, in the period of time from 40 to 80 μs, the zone, where $\varepsilon^p_{\text{eff}}$ = 0.14, is distributed over the thickness of the plate, changing its shape from a circular segment (40 μs) to a trapezoid one (60–80 μs). Within a period equal to 80 μs (Figure 3, *d*), on the reverse surface of the plate a local zone is formed, where $\varepsilon^p_{\text{eff}}$ = 0.24, which exceeds $\varepsilon^p_{\text{eff}}$ in the contact zone. Such a result can be explained by the inertial component of the process of interaction of two bodies, which in comparison with the impact-wave component has a significant advantage in this problem. As a result of contact, a part of the kinetic energy of the indenter is gradually transferred to the plate. After that, a compression wave is formed in it, which forces the layers of material to move vertically in the direction of the working table. Having met a rigid support on the way, the material of a plate repulses from it. Due to the fact that this process is not instantaneous, the first to stop are the layers of the plate material bordering on the working table. In the future, they will try to start their movement in the opposite direction. However, they are prevented from doing so by other moving layers of the plate material, which continue to approach the table. As a result, the boundary region of the plate becomes clamped between a fixed absolutely rigid table and a moving part of the plate material. Thus, the value $\varepsilon^p_{\text{eff}}$ receives an additional pulse to increase its value. Thus, at V_0 = 10 m/s a «repulsion effect» of the material layers on the reverse surface of the plate occurs, which are in contact with the rigid base 3 (Figure 2).

The residual calculated distribution of effective plastic deformations throughout the plate thickness at different values of the collision rate with the indenter-electrode is shown in Figure 4. From Figure 4 it is seen that the radius of the imprint on the surface of the plate from the interaction with the electrode-indenter almost corresponds to the width of the zone of plastic deformation *x* (Table 2) unlike the zone of plastic deformation on the reverse surface, which narrows over the thickness. Thus, the shape of the plastic deformation zone has the shape of a triangle. However, due to a «repulsion effect», the residual values on the reverse surface of the plate are higher than $\varepsilon^p_{\text{eff}}$ on the contact surface.

The kinetics of the values of the effective plastic deformation at the points of the plate located at different distances from the contact zone along the impact line, at different values of movement speed V_0 of the electrode-indenter, is presented in Figure 5. Thus, in the case of movement of the indenter at a speed V_0 = = 5 m/s (Figure 5, *a*), the maximum values $\varepsilon^p_{\text{eff}}$ are formed in the contact zone of the electrode-indenter and the plate (point *B*, Figure 2) , which are presented in Table 2. If V_0 = 10 m/s, then prior to *t* = 80 μs the maximum values $\varepsilon^p_{\text{eff}}$ are also formed in the place of contact of the electrode-indenter. However, after 80 μs this process changes significantly (Figure 5, *b*). From this moment, the value $\varepsilon^p_{\text{eff}}$ for the point located on the reverse surface of the plate (point *B*, Figure 2),

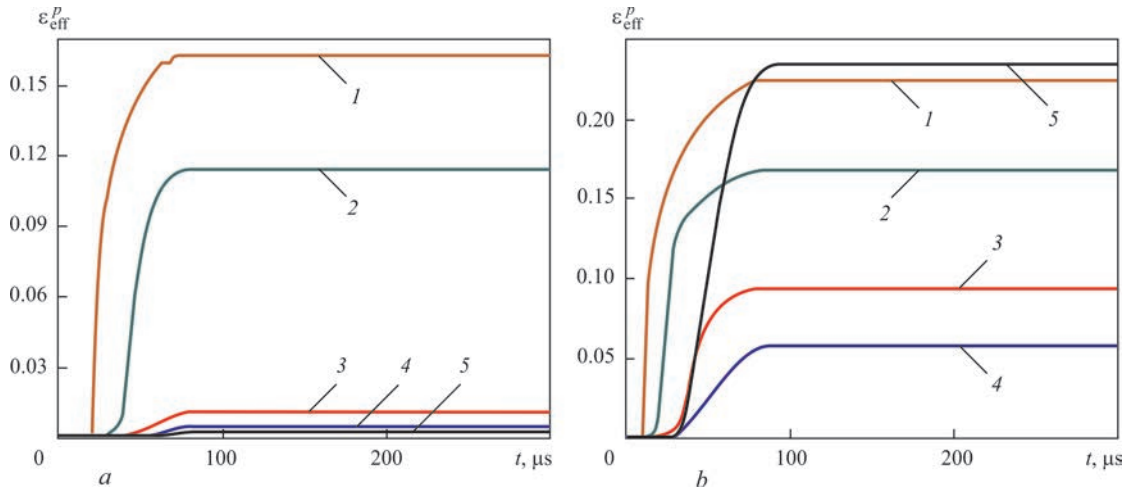

Figure 5. Variation of the values of effective plastic deformation ε^p_{eff} with time at the points of the plate, located at different distances from the contact point (mm: *1* — 0; *2* — 1; *3* — 2; *4* — 3; *5* — 4) along the impact line, at different values of speed of movement of the electrode-indenter, m/s: *a* — 5; *b* — 10

gradually starts exceeding the similar values for the point *B*. This can be explained by the «repulsion effect», the mechanism of which is given above.

At the same time, the dependences ε^p_{eff} (Figure 5) do not provide a possibility to evaluate a full picture of the deformed state of the plate, for example, the position of the zones of compression and tension.

Figure 6 presents the distribution of components of plastic deformation ε^p_x and ε^p_y. It can be seen that at a speed V_0 = 1 m/s the indenter has almost superficial effect on the plate material (which is confirmed by the data in Figure 4, *a*), in contrast to the interaction between the plate and the indenter, when the speed of the latter was 5 m/s (Figure 6, *c*, *d*) and 10 m/s (Figure 6, *d*, *e*), which confirms the data of Figure 4, *b*, c, at which ε^p_x and ε^p_y are distributed over the thickness of the plate.

At V_0 = 5 m/s, the values of the vertical component ε^p_y of plastic deformation exceed the values of the component ε^p_x. In this case, the values ε^p_y, which in the surface layers of the metal remain in the state of an intensive yield, are mainly compressive. The peak value of the component ε^p_y is –0.143. This also indicates the formation of a wide area of compression deformations. The distribution of the horizontal component ε^p_x is almost identical to ε^p_y, but only in the area close to the contact surface. As it passes into the middle of the plate along the impact line, the zone of compression deformations gradually turns from the value ε^p_x = –0.0134 to the zone of tensile deformation with a peak value in the center of the zone ε^p_x = 0.015.

If the indenter has a speed V_0 = 5 m/s, then the compression deformations of the vertical component ε^p_y have two extremes, the values of which are close to the plastic flow, but in fairly localized areas. The first is on the contact surface at the point *B* (Figure 2) at the value ε^p_y = –0.192, the second one is on the reverse surface (ε^p_y = –0.206) at the point *B* (Figure 2). At the same time, the value of the component ε^p_x on the contact surface is equal to 0.01, and on the reverse one it transfers into tensile deformation, which grows to the value ε^p_x = 0.196.

All these processes were reflected on the kinetics (changes over time) of the stress components in the plate at the value of the speed of the electrode-indenter V_0 = 5 m/s (Figure 7). It should be noted that kinetics of stresses at V_0 = 10 m/s is close to that shown in Figure 7.

From Figure 7 it is seen that the process of interaction of the indenter with the plate is accompanied by the formation of compressive stresses σ_y with the output of these values to the yield strength in the latter on the impact line. At the end of the contact between the bodies, the stresses σ_y fall to zero with the subsequent increase in the value on the plate surface to 75 MPa, if V_0 = 5 m/s (Figure 7, *b*) and to 50 MPa, if V_0 = 10 m/s. The change in the values σ_x has a multidirectional character. In the contact zone at V_0 = 5 and 10 m/s, in the plate compressive stresses with a value of up to –110 MPa are predominant, and at the distance from the zone of 4 mm, tensile stresses are formed. The superposition of compressive stresses (–110 MPa) in the plate, which are formed as a result of collision with the indenter with residual welding tensile stresses, the value of which can be 150 MPa, should provide a significant reduction of the latter to almost unstressed state. The interaction of tensile stresses (110 MPa) in the plate, which are formed as a result of the impact action of the indenter with the residual welding tensile stresses, the value of which can be 150 MPa, should provide an exceed in the yield strength of AMg6 al-

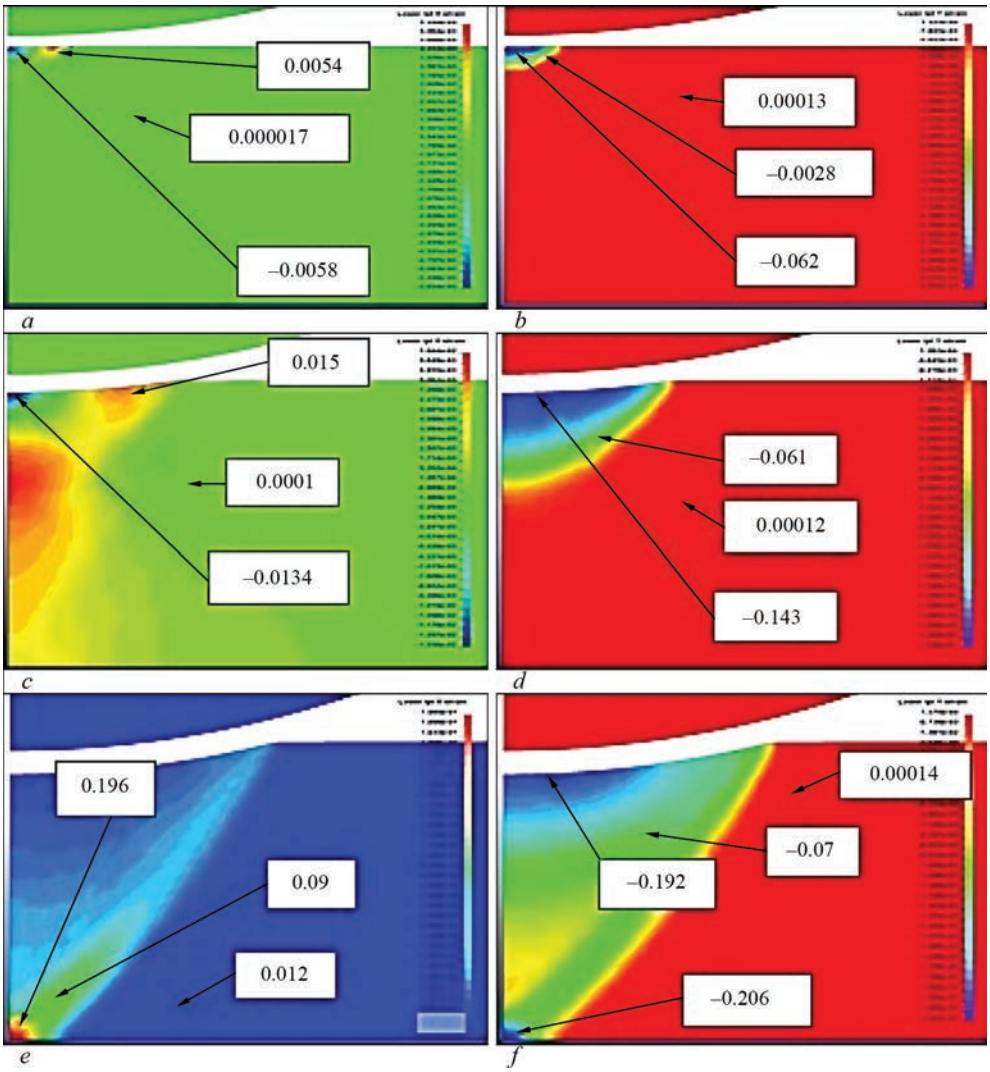

Figure 6. Residual calculated distribution of values of components of plastic deformations over the thickness of the plate at different values of the collision rate (m/s: *a*, *b* — 1; *c*, *d* — 5; *e*, *f* — 10) with the electrode-indenter: *a*, *c*, *e* — ε_x^p ; *b*, *d*, *f* — ε_y^p

loy, the result of which is transition of the deformed layer to the elastic-plastic state, where plastic tensile deformations dominate. This, as in the case of interaction of tensile and compressive stresses on the contact surface, should facilitate the reduction in the initial (before treatment) level of residual tensile stresses.

Figure 8 shows the corresponding residual calculated distribution of stress components σ_x and σ_y at

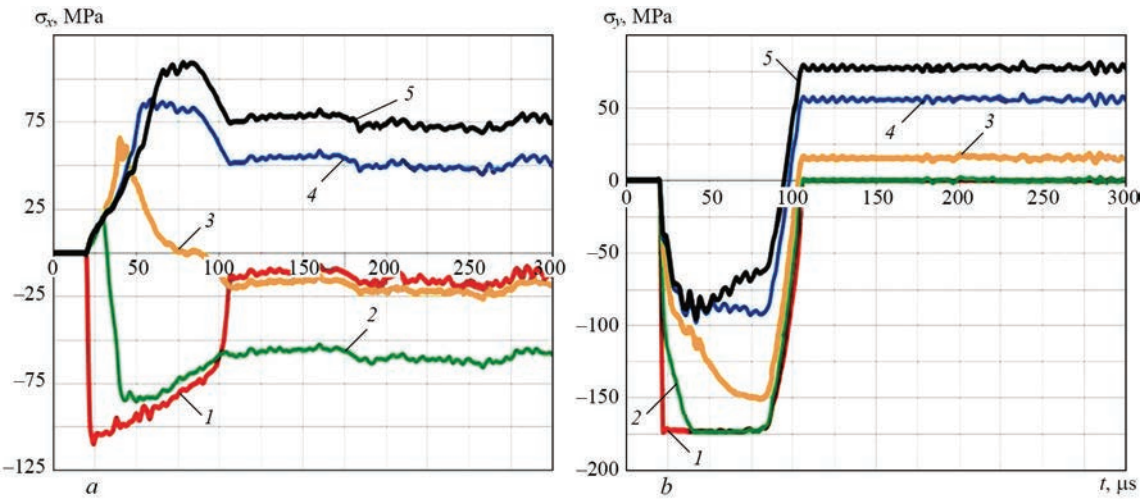

Figure 7. Diagrams of variation of the values of horizontal σ_x (*a*) and vertical σ_y (*b*) components of stresses with time in the points of the plate, located at different distances from the contact zone (mm: *1* — 0; *2* — 1; *3* — 2; *4* — 3; *5* — 4) along the impact line according to the value of the speed of movement of the indenter V_0 = 5 m/s

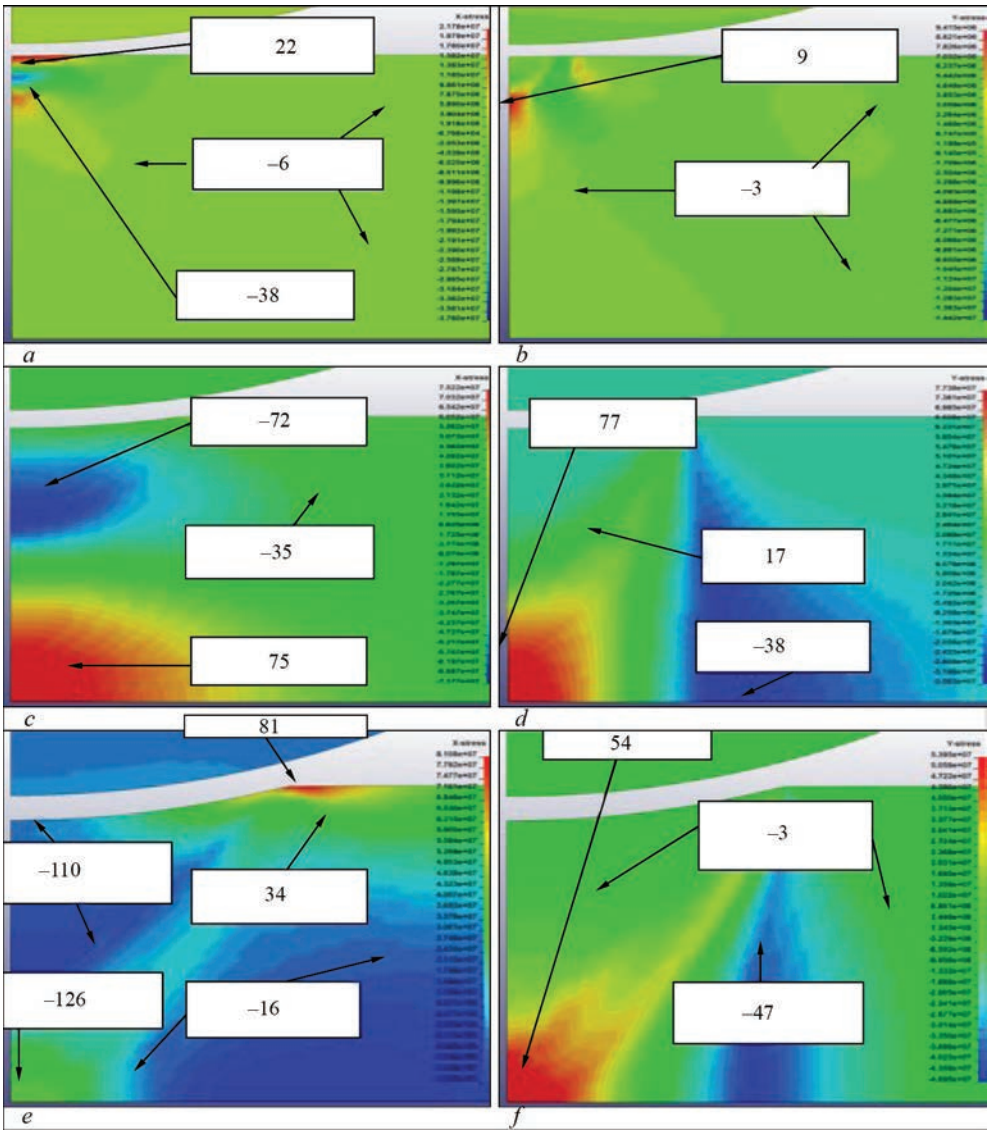

Figure 8. Calculated distribution of the components of the residual stresses (MPa) in the middle of the plate at different speed values (m/s: *a*, *b* — 1; *c*, *d* — 5; *e*, *f* — 10) collision with the electrode-indenter: *a*, *c*, *e* — σ_x; *b*, *d*, *f* — σ_y

different values of the collision rate with the indenter electrode. At a speed V_0 = 1 m/s, the zone of influence of the indenter is quite localized, and the average values of σ_x and σ_y over the thickness of the plate reach –6 and –3 MPa, respectively.

At an impact speed V_0 = 5 m/s moving further from the collision line in the horizontal direction *x*, the zone of tensile stresses σ_y gradually changes with the compression zone with the subsequent transition to the unstressed state.

In addition, the line of transition of stresses σ_y from tension to compression at V_0 = 5 m/s has an almost vertical location.

If the speed grows to 10 m/s, the transition of σ_y to the zero value occurs after the repeated transition of the function to the region of tensile stresses. In this case, the line of transition between the zones of compression and tension (unlike the line of transition between the zones at a speed V_0 = 5 m/s) is inclined at an angle of 75°. At V_0 = 10 m/s, the compressions, the values of which reach –47 MPa, are localized at the edge of the contact zone and developed over the thickness of the specimen. They are balanced by tensile σ_y, which are localized over the thickness of the specimen and reach up to 54 MPa.

It can be seen that the contact of the indenter at a speed V_0 = 1 m/s does not cause significant changes in the component σ_x of the stress state over the thickness of the plate. The introduction at V_0 = 5 m/s provides the value of compressive σ_x in the contact zone at the surface of the plate to –72 MPa, which are compensated by tensile σ_x = 75 MPa near the reverse surface of the specimen. The zone of compression impact up to σ_x = –35 MPa is much larger, which is distributed almost along the entire thickness of the plate in the zone close to the impact line. Another distribution of σ_x occurs at V_0 = 10 m/s, where at the outer and reverse surfaces the compressive stresses σ_x predominate, ranging from

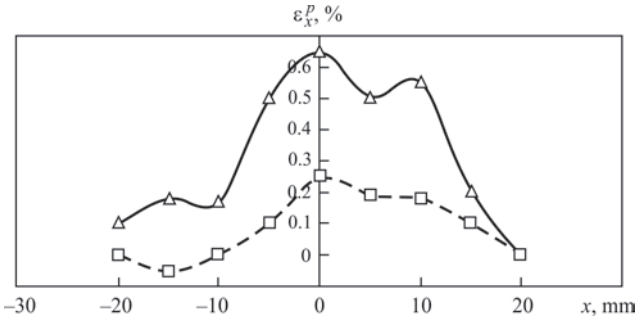

Figure 9. Distribution of longitudinal component of plastic deformations ε_x^p on the surfaces *B* and *C* (Figure 2) of the annealed plate and AMg6 alloy after impact action on the surface *B* at V_0 = = 10 m/s along the IL, where *X* = 0

–110 to –126 MPa, respectively, distributed over the thickness of the plate, which qualitatively confirms the effect of repulsion of plastically deformed layers of the plate at V_0 = 10 m/s. At the edge of the contact zone (σ_x = 81 MPa) of tension localized in a small area do not significantly affect the overall stress state of the plate due to its contact with the indenter.

When comparing the distributions of σ_x at V_0 = 5 and 10 m/s, it can be seen that the maximum values of the component σ_x of compressive stresses are reached at V_0 = 10 m/s in the outer surface layers along the impact line. At V_0 = 10 m/s, the areas of compressive stresses σ_x are distributed over a larger cross-sectional area of the plate (as compared to σ_x at V_0 = 5 m/s).

To evaluate the adequacy of modeling, the distribution of the longitudinal component of the plastic deformations ε_x^p on the surfaces *B* and *C* (Figure 2) of the annealed plate of AMg6 alloy with the dimensions of 400×360×4 mm was experimentally investigated. The mode of heat treatment of the plate included the presence of any initial stresses in the metal. EDT of the surface *B* was performed on a mode, whose electrophysical parameters correspond to the value V_0 = 10 m/s. Distributions of ε_x^p, which are shown in Figure 9, were recorded according to the procedure using a strain gauge with a measurement base B_d = 25 mm [15]. It can be seen that the impact action is distributed along the cross-section of the plate, and the values of ε_x^p on the side *B* (opposite contact) are higher than ε_x^p on the side *B* (contact). The dominant effect of EDT is observed over the width of the plate (along the line *X*) on the side opposite to the treatment. This qualitatively confirms the results of modeling presented in Figure 7, and allows making a conclusion that the result of the interaction of metal layers moving in opposite directions along the impact line (IL) is the «repulsion effect», the mechanism of which is described above. The result of the «repulsion effect» is an increased level of residual deformations ε_x^p on the surface opposite to the treatment.

Comparison of the results of modeling (Figure 7) and the experiment (Figure 9) was performed on the surfaces of plates *B* and *C* (Figure 2). It can be seen that on the reverse surface *B*, the calculated and experimentally determined values ε_x^p near the impact line reach 1.2 and 0.65 %, respectively, and 0.6 and 0.25 %, respectively, on the contact *B*, i.e., they differ approximately twice. Thus, those calculated values ε_x^p predominate, which were obtained experimentally. The discrepancy between the results can be explained not by taking into account the evolution of the mechanical characteristics of the AMg6 alloy due to the action of a pulsed current with a density $\geq$ 1.0 kA/mm^2, i.e. realization of the electroplasticity effect [4, 5]. Taking into account the effect of the pulsed current on the stress-strained state of the AMg6 alloy during EDT is presented in [16].

Also, the difference between the results of modeling and experimental evaluation of the distribution of deformations along the impact line is explained by the fact that the values ε_x^p obtained by the method of mechanical tensometry, are averaged along the length of B_d. This results in smaller experimental values ε_x^p as compared to those, calculated on the basis of the model.

Analyzing the general results of stress state calculations when comparing them with the experimental data given in [4, 5], it can be noted that modeling allows predicting the stress-strain state of a welded plate, which is the result of its interaction with a hemispherical indenter. Moreover, the contact speed is set by the electrophysical parameters of electrodynamic treatment. This allows optimizing the parameters of the EDT mode of a wide range of metals, alloys and welded joints in order to minimize their stress-strain state.

Conclusions

1. A mathematical model of the influence of the impact action of the electrode-indenter on the stress-strain state of an unstressed plate of aluminium AMg6 alloy during its electrodynamic treatment was developed.

2. On the basis of numerical analysis of the process of impact interaction of the electrode-indenter with the plate, the parameters of the stress-strain state were obtained, which can contribute to the reduction of residual stresses in the weld.

3. If the speed of movement of the elecdtrode-indenter grows to 10 m/s, then on the reverse surface of the plate, the value of the effective plastic deformation begins to exceed similar values on the contact surface.

4. The superposition of compressive stresses in the plate, which are formed as a result of collision with the electrode-indenter, with the residual welding tensile stresses should provide a significant reduction of the latter.

5. Experimental studies of distributions of plastic deformations on the outer and reverse surfaces of the plate of AMg6 alloy as a result of impact action at a speed of movement of the electrode-indenter of 10 m/s qualitatively confirmed the adequacy of modeling.

1. Masubuchi, K. (1980) *Analysis of welded structures*. Pergamon Press.
2. Lashchenko, G.I., Demchenko, Yu.V. (2008) *Energy-saving technologies of postwelding treatment of metal structures.* Kiev, Ekotekhnologiya [in Russian].
3. Lobanov, L.M., Pashin, N.A., Mihoduy, O.L., Khokhlova, J.A. (2016) Investigation of residual stress in welded joints of heat-resistant magnesium alloy ML10 after electrodynamic treatment. *J. of Magnesium and Alloys*, **4**, 77–82.
4. Lobanov, L.M., Pashin, N.A., Mihoduy, O.L. (2014) Repair the AMr6 aluminium alloy welded structure by the electric processing method. *Weld Research and Application*, **1**, 55–62.
5. Lobanov, L.M., Pashin, N.A., Mikhodui, O.L., Sidorenko, Yu.M. (2018) Electric pulse component effect on the stress state of AMg6 aluminium alloy welded joints under electrodynamic treatment. *Strength of Materials*, 50(**2**), 246–253. ttps://doi.org/10.1007/s11223-018-9965-x.
6. Lobanov, L.M., Pashchin, N.A., Timoshenko, A.N. et al. (2017) Effect of the electrodynamic treatment on the life of AMg6 aluminium alloy weld joint. *Ibid.*, 49(**2**), 234–238. http://dx.doi.org/10.1007/s11223-017-9862-8
7. Sidorenko, Yu.M., Shlenskii, P.S. (2013) On the assessment of stress–strain state of the load-bearing structural elements in the tubular explosion chamber. *Ibid.*, 45(**2**), 210–220.
8. http://www.ansys.com/
9. http://www.ls-dyna.ru/
10. Mujzemnek, A.Yu., Bogach, A.A. (2005) *Mathematical modeling of shock and explosion processes in LS-DYNA program:* Manual. Penza, Inform. Izd. Tsentr PGU [in Russian].
11. Babkin, A.V., Kolpakov, V.I., Okhitin, V.N. et al. (2000) *Numerical methods in problems of explosion and shock physics.* In: Manual for higher educ. instit. Ed. by V.V. Selivanov. Moscow, MGTU, Vol. 3 [in Russian].
12. Rudakov, K.M. (2007) *Numerical methods of analysis in dynamics and strength of structures. In: Manual.* Kyiv, NTUU KPI [in Ukrainian].
13. Odintsov, V.A., Sidorenko, Yu.M. (2001) Modeling of the explosion process of standard fragmentation cylinder with varying degrees of detail. *Oboronnaya Tekhnika*, **1–2**, 17–20 [in Russian].
14. Lobanov, L.M., Pashin, N.A., Mykhodui, O.L., Sydorenko, Yu.M. (2017) Effect of the indenting electrode impact on the stress-strain state of an AMg6 alloy on electrodynamic treatment. *Strength of Materials*, 49(**3**), 369–380. DOI: https://doi.org/10.1007/s11223-017-9877-1
15. Kasatkin, B.S., Prokhorenko, V.M., Chertov, I.M. (1987) *Welding stresses and strains.* Kiev, Vyshcha Shkola [in Russian].
16. Sydorenko, Y.M., Pashchyn, M.O., Mykhodui, O.L. et al. (2020) Effect of pulse current on residual stresses in AMg6 aluminium alloy in electrodynamic treatment. *Strength of Materials*, 52(**5**), 731–737. DOI: https://doi.org/10.1007/s11223-020-00226-2

Received 26.03.2021